Particle-Scale Modeling of Coal Devolatilization Behaviors for Coal Pyrolysis in Thermal Plasma Reactors

Binhang Yan, Yan Cheng, and Yi Cheng
Dept. of Chemical Engineering, Beijing Key Laboratory of Green Chemical Reaction Engineering and Technology, Tsinghua University, Beijing 100084, P.R. China

DOI 10.1002/aic.14698
Published online December 8, 2014 in Wiley Online Library (wileyonlinelibrary.com)

A generalized heat transfer and devolatilization model coupled with the thermal balance between the heating gas and particles was established to predict the complex coal pyrolysis behaviors in the practical plasma reactors. It was proved that this model could well describe the coal devolatilization behaviors in both the pilot-scale and lab-scale plasma reactors as the mechanisms of coal chemistry and particle-scale physics were incorporated. The achieved understanding on the reactor energy balance demonstrated that the heat recovery of the quenching process was crucial to the thermal efficiency and economic benefit of the overall project. The in-depth discussion of the influences of coal feed rate and particle size on the reactor performance revealed the dominant roles and presented the optimal values of these two factors. In particular, the simulation results of several coals could help to provide a simple, quick method of coal type selection for industrial plasma processes. © 2014 American Institute of Chemical Engineers *AIChE J*, 61: 913–921, 2015
Keywords: coal, devolatilization, modeling, thermal plasma, heat transfer

Introduction

Coal pyrolysis in thermal plasma, which is known as a highly efficient coal conversion technique to chemicals and alternative fuels, would open up a direct and cleaner means for producing acetylene (C_2H_2).[1,2] This novel acetylene production technique was first discovered by Bond et al.[3] using a plasma jet in the early 1960s. When pulverized coal particles were injected into the thermal plasma jet, the volatiles would be released rapidly and soon converted to acetylene at such high temperature, nonoxidative atmosphere. As then, research on coal pyrolysis in thermal plasma has attracted world-wide attention.[4–9] It is worth mentioning that the largest plasma reactors for coal pyrolysis at industrial demonstration scale (i.e., 2000 and 5000 kW power input) in the world have been successfully built, operated continuously and stably for more than 75 h per run in China.[1,10]

Different from other coal conversion techniques, the performance of this process is principally dominated by the yield of total volatiles (which is greatly dependent on coal type). As the process is operated under extreme conditions such as ultrahigh temperature (e.g., ~3000 K) and milliseconds contact time, the coal type selection, operating conditions optimization, and reactor scale-up are actually very difficult to be achieved only through a large number of experiments. Besides, the particle heating history and volatiles evolution would interact strongly with each other during pyrolysis. Therefore, it is important to establish a theoretic model incorporating the mechanisms of coal chemistry and particle-scale physics to enable reasonable predictions on coal pyrolysis behaviors in such a severe environment so as to provide scientific guidance for the coal type selection and operating conditions optimization of industrial plasma process.

In our previous work,[11] a heat transfer and devolatilization model incorporating the particle-scale physics was established to understand the heat transport and pyrolysis behavior inside a single coal particle. The results showed that both the inherent heat-transfer resistances and endothermic heat of devolatilization would lead to a large temperature gradient/difference within particle, especially when the particle size was large or the intensity of heat transfer between the surrounding gas and particles was strong. All these factors impeded thermal energy from transporting into the particle, leading to a weakened heating-up rate and thereafter a longer devolatilization time. Therefore, these particle-scale physics inside particle should be paid enough attention to for such an ultrahigh temperature and ultrafast pyrolysis process. The chemical percolation devolatilization (CPD) model,[12–14] which was originally developed by Grant et al.[12] to model coal devolatilization based on the characteristics of the chemical structure of the parent coal, was used for its wide applicability.[15,16] The coal-independent kinetic parameters were refitted, and the coal-dependent structure parameters were adjusted according to the experimental data,[11] so that the predictive accuracy of the CPD model was markedly raised, indicating that this model was applicable to describe the devolatilization behaviors of various coal types under different conditions.

However, the simulations in the previous work[11] were based on the assumption that the effect of the discrete particles on the surrounding gas was ignored, that is, the

Correspondence concerning this article should be addressed to Y. Cheng at yicheng@tsinghua.edu.cn.

temperature, components, and properties of the heating gas were assumed to be unchangeable during pyrolysis. As a consequence, the established model can be only used to reveal the devolatilization behavior of a single particle under the designed conditions where the mass fraction of coal particles is extremely low. In a practical coal conversion process, the mass flow rate of coal particles is usually several times of the mass flow rate of thermal plasma.[17–19] The temperature, components as well as the thermodynamic and transport properties of the heating gas will change significantly once the devolatilization reactions occur, resulting in different coal pyrolysis behaviors.

Therefore, the generalized heat transfer and volatiles evolution model coupled with the thermal balance between the heating gas and coal particles, that is, taking the interaction between the heating gas and particles into account, was established to deepen the understanding of the complex coal pyrolysis behaviors in the practical plasma reactors in this work. The model predictions were validated with the experimental data under the typical operating conditions from both the 2000 kW pilot-scale and 10 kW lab-scale plasma reactors. Then, the overall energy balances and the particle-scale behaviors of both reactors were analyzed. Furthermore, the effects of coal feed rate and particle size on the performance of pilot-scale plasma reactor were discussed to obtain the optimal operating conditions. Finally, the devolatilization performances of several coals under the operating conditions from the pilot-scale reactor were performed, providing scientific guidance for the coal type selection of industrial plasma process.

Mathematical Model

Model assumptions

To incorporate the influence of the discrete particles on the surrounding gas, some basic simplifications and assumptions, besides those shown in the previous work,[11] were made as following:

1. The particles are assumed to be ideally mixed with the carrier gas in thermal plasma.

2. The fragmentation, swelling, and shrinkage of coal particles are ignored. According to the work of Shurtz et al.,[20] particle swelling does not occur significantly for low rank coals or for bituminous coals when the particle heating rate is high enough (over $\sim 10^5$ K/s). Therefore, the particle swelling can be reasonably ignored as the particle heating rate in rapid plasma pyrolysis process is usual in the ranger of 10^4–10^6 K/s.[2,11,21] As an alternative approach, the particle volume is assumed constant while the porosity of particle is varying during pyrolysis in this work.

3. The coking phenomenon and the gas-phase chemical reactions are ignored. The performance of this process is principally dominated by the yield of total volatiles (i.e., coal conversion, which is greatly dependent on coal type) and the composition of volatiles.[11] Therefore, special attention is focused on the detailed devolatilization behavior (i.e., particle heating history and coal conversion) in this work. From this perspective, ignoring coking phenomenon would have almost no impact on the particle heating history and coal devolatilization. As the heat effect of the cracking of hydrocarbons to acetylene is quite noticeable, the kinetics calculation of the numerous complex gas-phase reactions is ignored but the heat of hydrocarbons pyrolysis is considered to be included in the "virtual" heat of devolatilization as an alternative approach. The "virtual" heat of devolatilization is calculated based on the standard formation enthalpies of coal, char, and volatiles in which acetylene is assumed to be the principal hydrocarbon component. The standard formation enthalpies of coal and char are estimated based on the calorific value measurements of the parent coal and the char after pyrolysis. Even so, it is anticipated that detailed gas-phase chemical reactions together with the corresponding heat effects would be further incorporated in this model for modeling coal pyrolysis in the practical plasma reactors.

4. The particle–particle interactions, as well as the collision and radiation between particles and reactor wall, are neglected. Due to the fairly low particle volume fraction (which is far below 1%) and the much larger temperature difference between the heating gas and the wall compared to that between the particles and the wall, the heat loss to the wall is dominated by the convective and radiative heat flux between the heating gas (plasma) and the wall, rather than the radiative heat flux between the particles and the wall. Therefore, the radiation between the particles and the reactor wall is neglected while the convective and radiative heat transfer between the heating gas and the wall is paid special attention to.

5. The temperature of reactor wall is assumed to be constant, both the radiative heat transfer and the convective heat transfer between the gas and reactor wall are taken into account.

6. The gas temperatures on each cross-section of reaction chamber at each time step are assumed to be the same due to the strong turbulence intensity in the reactor.

Heat-transfer model inside a particle

Based on our earlier work,[11] the heat-transfer model inside a particle, including the contributions from convection, radiation, and the heat consumed during devolatilization, can be written as

$$\left(\rho_{\mathrm{p}} c_{\mathrm{p}}\right)_{\mathrm{eff}} \frac{\partial T_{\mathrm{p}}(r,t)}{\partial t} = \frac{1}{r^2}\frac{\partial}{\partial r}\left(\lambda_{\mathrm{eff}} r^2 \frac{\partial T_{\mathrm{p}}(r,t)}{\partial r}\right) - \Delta_{\mathrm{r}} H \cdot \gamma_{\mathrm{vol}}(r,t) \tag{1}$$

where, r is radial position, t is time, T_{p} represents the local temperature; ρ_{p} and c_{p} are the effective local density and specific heat capacity, respectively; λ_{eff} is the effective local thermal conductivity; $\Delta_{\mathrm{r}}H$ is the heat of devolatilization (J/kg), γ_{vol} denotes to the rate of devolatilization (kg/m^3 s), which is calculated from the CPD model.[11]

The initial condition is:

$$T_{\mathrm{p}}(r,0) = T_{\mathrm{p,init}} \quad (0 \le r \le R) \tag{2}$$

R is the particle radius and $T_{\mathrm{p,init}}$ is the initial particle temperature (typically set to 300 K).

The boundary conditions are:

$$\begin{cases} 4\pi R^2 \lambda_{\mathrm{eff}} \dfrac{\partial T_{\mathrm{p}}}{\partial r}\Big|_{r=R} = 4\pi R^2 h\left(T_{\mathrm{g}} - T_{\mathrm{w}}\right)\theta + \sigma(4\pi R^2)\left(\varepsilon_{\mathrm{g}} T_{\mathrm{g}}^4 - \varepsilon_{\mathrm{p}} T_{\mathrm{W}}^4\right) \\ \dfrac{\partial T_{\mathrm{p}}}{\partial r}\Big|_{r=0} = 0 \end{cases} \tag{3}$$

The subscripts g, w, and p denote the heating gas, the surface of particle and the particle, respectively; h is the gas–particle heat-transfer coefficient; σ is the Stefan–Boltzmann

constant; ε is the black-body radiation coefficient; and θ, reported by Spalding,[22] is an effective particle-based correction for considering the heat-transfer resistance due to the fast release of volatiles. When the release of volatiles occurs, $\theta < 1$, and the smaller the θ is, the larger the effect of volatiles diffusion on heat transfer is.

Heat exchange between heating gas and coal particles

The heat exchange between heating gas and a particle at each time step is computed as

$$Q_{\text{gas-particle}} = Q_{\text{conv,p}} + Q_{\text{radi,p}} \tag{4}$$

where

$$Q_{\text{conv,p}} = \theta h(4\pi R^2)\left(T_{\text{g}} - T_{\text{w}}\right)\Delta t \tag{5}$$

$$Q_{\text{radi,p}} = \sigma(4\pi R^2)\left(\varepsilon_{\text{g}} T_{\text{g}}^4 - \varepsilon_{\text{p}} T_{\text{W}}^4\right)\Delta t \tag{6}$$

In these equations, $Q_{\text{conv,p}}$ and $Q_{\text{radi,p}}$ are the convective heat-transfer quantity and radiative heat-transfer quantity between heating gas and a particle, respectively; Δt is time step.

Heat exchange between heating gas and reactor wall

The heat exchange between heating gas and the wall of reaction chamber at each time step is computed as

$$Q_{gas-wall} = Q_{\text{conv,wall}} + Q_{\text{radi,wall}} \tag{7}$$

where

$$Q_{\text{conv,wall}} = h_{\text{wall}}\left(2\pi R_{\text{reactor}} U_{\text{g}}\right)\left(T_{\text{g}} - T_{\text{wall}}\right)\Delta t \tag{8}$$

$$Q_{\text{radi,wall}} = \sigma\left(2\pi R_{\text{reactor}} U_{\text{g}}\right)\left(\varepsilon_{\text{g}} T_{\text{g}}^4 - \varepsilon_{\text{wall}} T_{\text{wall}}^4\right)\Delta t \tag{9}$$

In these equations, $Q_{\text{conv,wall}}$ and $Q_{\text{radi,wall}}$ are the convective heat-transfer quantity and radiative heat-transfer quantity between heating gas and reactor wall, respectively; R_{reactor} is the radius of the reaction chamber; U_{g} is the average velocity of the heating gas.

Heat balance equations

The heat balance equation of a particle at each time step is:

$$Q_{\text{conv, p}} + Q_{\text{radi, p}} = \Delta H_{\text{char}} + Q_{\text{devol}} + \tilde{H}_{\text{vol}} \tag{10}$$

where

$$\Delta H_{\text{char}} = \int_0^R \left(\rho_{\text{char}}^1 H_{\text{char}}^1 - \rho_{\text{char}}^0 H_{\text{char}}^0\right) 4\pi r^2 dr \tag{11}$$

$$Q_{\text{devol}} = \int_0^R \left(\Delta_{\text{r}} H \cdot \gamma_{\text{vol}}\right) 4\pi r^2 dr \Delta t \tag{12}$$

$$\tilde{H}_{\text{vol}} = \int_0^R \left(H_{\text{vol}} \cdot \gamma_{\text{vol}}\right) 4\pi r^2 dr \Delta t \tag{13}$$

where, H is the enthalpy, Q_{devol} represents the heat of devolatilization, $\tilde{H}_{\text{vol}}$ is the total enthalpy/energy carried in the volatiles released during this time step; the subscripts char and vol represent the solid residue and the volatiles, respectively; the superscripts 0 and 1 represent the last time step and the current time step, respectively. The temperature of the volatiles just released is assumed to be the same with the temperature of the char (coal residue) at any local position inside the particle.

For an open system in which some of the energy exchange (without work) is brought about by the flow of mass across the system on boundaries, the energy balance[23] is

$$\frac{dE_{\text{sys}}}{dt} = Q + F_{\text{in}} E_{\text{in}} - F_{\text{out}} E_{\text{out}} \tag{14}$$

where, $\frac{dE_{\text{sys}}}{dt}$ is the rate of accumulation of energy within the system, Q is the rate of flow of heat to the system from the surroundings, $F_{\text{in}}E_{\text{in}}$ is the rate of energy added to the system by mass flow into the system, $F_{\text{out}}E_{\text{out}}$ is the rate of energy leaving system by mass flow out of the system.

At each time step, the heat balance equation of the heating gas can be written as

$$\dot{m}_{\text{gas}}^0 H_{\text{gas}}^1 - \dot{m}_{\text{gas}}^0 H_{\text{gas}}^0 = \left(N_{\text{p}} \tilde{H}_{\text{vol}} - N_{\text{p}} Q_{\text{gas-particle}} - Q_{\text{gas-wall}}\right) + 0 - \dot{m}_{\text{vol}} H_{\text{gas}}^1 \tag{15}$$

Let $\dot{m}_{\text{gas}}^1 = \dot{m}_{\text{gas}}^0 + \dot{m}_{\text{vol}}$, then

$$\dot{m}_{\text{gas}}^0 H_{\text{gas}}^0 - \dot{m}_{\text{gas}}^1 H_{\text{gas}}^1 = N_{\text{p}}\left(Q_{\text{gas-particle}} - \tilde{H}_{\text{vol}}\right) + Q_{\text{gas-wall}} \tag{16}$$

where

$$H = \int_{T_{\text{ref}}}^{T} c_{\text{p}} dT + h^0(T_{\text{ref}}) \tag{17}$$

In these equations, $\dot{m}_{\text{gas}}$ represents the mass flow rate of the heating gas; N_{p} is the number of particles, $N_{\text{p}}\tilde{H}_{\text{vol}}$ is the total energy carried to the system by the volatiles released, $N_{\text{p}}Q_{\text{gas-particle}}$ is the total energy from the heating gas to the particles, $Q_{\text{gas-wall}}$ is the total energy from the heating gas to the wall. $h^0(T_{\text{ref}})$ is the formation enthalpy at the reference temperature T_{ref}. In calculation of the enthalpies, the temperature of the volatiles outside a particle is assumed to be simultaneously raised to the temperature of the heating gas. Here, the volatiles instantaneously reach the gas temperature means ignoring the mixing time but not the enthalpy change. The temperature of the mixture (i.e., the plasma gas and the volatiles) is calculated based on the energy balance under the assumption that the temperatures of the volatiles and the gas are the same after they are mixed.

Physicochemical properties and numerical solution

During the simulation, the physicochemical properties of coal/char are estimated as a function of local position and temperature.[24,25] The properties of the heating gas are calculated by user-defined mixing law as a function of its components and temperature. The heating gas consists of plasma and volatiles. The physical properties of plasma gas are given from Boulos et al.[26] as a function of components and temperature. The material properties of the volatiles, which are treated as a gas mixture, are obtained by kinetic theory method.[27] The temperature, components, and properties of the heating gas are updated at each time step.

The heat-transfer equation (Eq. 1) is solved by an implicit integral finite volume method. The heat balance equation of the heating gas and the mass loss equation are solved by stepwise integration over discrete time steps. The particle is divided into 20 shells equally spaced along the radial direction. The time-step size is automatically adjusted according to the release rate of volatiles to guarantee good convergence. The coupled two-phase simulation is accomplished by alternately calculating these equations for heat/mass transfer

Table 1. Typical Operating Conditions of Both the Pilot-Scale and Lab-Scale Experiments

Operating Conditions	Unit	Pilot-Scale[2]	Lab-Scale[19]
Power input	kW	1800	2.0
Energy conversion efficiency	%	70	60
Internal diameter of reactor	m	0.080	0.014
Reactor length for pyrolysis	m	0.50	0.040
Temperature of reactor wall	K	500	400
Hydrogen feed rate (plasma torch)	kg/h	35	1.53
Methane feed rate (plasma torch)	kg/h	40	0
Hydrogen/argon feed rate (coal inlets)	kg/h	10	0.064
Coal feed rate	kg/h	700	0.12
Mean particle diameter	μm	50	50
Initial temperature of particles	K	300	300

to/from particles until both the mass and temperature of the heating gas and particle no longer change with further calculations.

Results and Discussion

Model validation

Two cases of coal pyrolysis experiments, which were carried out in the pilot-scale (i.e., 2000 kW power input) plasma reactor[2] and in the lab-scale (i.e., 10 kW power input) plasma reactor[19], respectively, were used to validate the reliability of this two-way coupling mechanism model as the gas–particle mixing efficiencies of both cases were considered to be excellent. Both reactors were composed of the plasma torch, mixing section, reaction chamber, quench device, and separator. The plasma-forming gas of the pilot-scale reactor was pure hydrogen while that of the lab-scale reactor was argon–hydrogen mixture. An extra hydrogen/argon gas introduced into the reactor was used to convey and accelerate coal particles. The typical operating conditions of both the pilot-scale and lab-scale experiments are shown in Table 1. The high volatile bituminous coal (Coal #1) originated in Xinjiang is used in both experiments. It is dried at 105°C for several hours and then stored in sealed containers. The analytical data of Coal #1 is presented in Table 2. The coal-dependent chemical structure parameters of Coal #1 for the CPD model are shown in Table 3.

The predicted coal conversions and average gas temperatures at the reactor outlet (we assumed the exit of the reaction chamber as the "outlet," not the actual outlet of the reactor) of both cases are plotted in Figure 1, together with the corresponding experimental data and thermodynamic analysis results.[28] It can be seen from Figure 1 that the model predictions agree well with the experimental data at both the lab-scale power input of 2 kW and pilot-scale power input up to 1800 kW. The mean residence time, which is estimated based on the volume of the reaction chamber, is about 1.3 ms for the pilot-scale reactor and 2.1 ms for the lab-scale reactor, respectively. The initial average gas temperatures (i.e., hydrogen/argon plasma before mixing with the coal particles) of the lab-scale and pilot-scale reactors are 3492 and 3236 K respectively. The average gas temperatures at the outlet of these two reactors are 1759 and 1886 K, respectively which are consistent with the quench temperature evaluated by the thermodynamic approach.[28] Therefore, this two-way coupling model is capable of describing the complex coal pyrolysis behaviors in the practical plasma reactors (in which the gas–particle mixing efficiencies should be good) under a wide range of operating conditions.

Energy balance and particle-scale behaviors

The overall energy balances around the reaction chamber of both reactors are shown in Figure 2. The heat loss of the plasma torch is quite high as it is made of water cooled copper. Thus the thermal efficiencies of the lab-scale and pilot-scale plasma torches are reasonably assumed to be 60 and 70%, respectively according to the corresponding experimental data. It can be seen from Figure 2 that the heat loss from the wall of the reaction chamber in the lab-scale reactor is much higher than that in the pilot-scale reactor. This is due to the smaller volume to surface area ratio of the lab-scale reactor. Therefore, in commercial operation the reactor should be designed with a larger volume to surface area ratio for a lower heat loss. The pyrolysis heat shown in Figure 2 means the amount of energy input used for the devolatilization reaction. It varies by the operating conditions (especially the mass flow rate ratio of coal to plasma) and the type of plasma reactor. The percentage of pyrolysis heat in total power input is very low in the lab-scale reactor because the mass flow rate ratio of coal particles to heating gas is quite low. It is worth mentioning that the total heat content of products (including the gas enthalpy and char enthalpy) before quenching in the pilot-scale reactor is fairly high (as high as 51% of total power input in the pilot-scale reactor). This suggests that the heat recovery and the energy cascade utilization of the quenching process are crucial to improve the thermal efficiency and economic benefit of the overall project for converting coal to chemicals.

The heat-transfer quantity from gas to coal particles is about 40.7% of total power input in the pilot-scale reactor, which consists of 39.2% convective heat-transfer quantity and only 1.5% radiative heat transfer quantity. The same phenomenon occurs in the lab-scale reactor, although the heat-transfer quantity is only 7.3% of total power input. Both cases indicate that the radiative heat transfer from gas to particles can be ignored under such operating conditions. However, the convective and radiative heat-transfer quantities from gas to the wall of reaction chamber are 3.3 and 1.1%, respectively in the lab-scale reactor, and even 10.4 and 20.1%, respectively in the pilot-scale reactor. This shows that radiation might dominate the heat transfer between gas and the wall, and should be paid enough attention to.

Figure 3 shows the variations of the maximum temperature difference and coal conversion difference inside particle as a function of residence time under the typical operating conditions from the pilot-scale and lab-scale plasma reactors. It can be obviously seen that the temperature/conversion gradient inside particle is quite significant in both the pilot-scale and lab-scale reactors: the peak values of the maximum temperature difference and coal conversion difference inside particle are as high as 1331 K (time = 0.16 ms) and 45.33 wt % (time = 0.38 ms), respectively in the former reactor, and the corresponding values are 1415 K (time = 0.27 ms) and 46.33 wt % (time = 0.42 ms), respectively in the latter case. Therefore, it should be noted that the inherent resistances (due to heat conduction and volatiles diffusion) cannot be ignored in a practical plasma reactor as the intensity of heat transfer is fairly strong, which is in accordance with our previous results.[11]

The radial profiles of the local temperature and mass loss (i.e., coal conversion) inside particle at any time can be

Table 2. Chemical Analyses of Coals

Coals			Proximate Analysis, wt %				Ultimate Analysis, wt %				
Origin	Name	Number	M_{ad}	A_d	V_d	FC_d	C_{daf}	H_{daf}	O_{daf}	N_{daf}	S_{daf}
Xinjiang	Heishan coal	#1	3.58	17.76	32.86	49.38	76.77	4.89	17.49	1.55	0.58
Xinjiang	Xinjiang coal	#2	3.66	15.18	34.61	50.21	76.49	4.85	17.20	1.54	0.53
Xinjiang	Miquan coal	#3	3.60	12.20	37.92	49.88	78.28	5.21	14.09	1.69	0.74
Inner Mongolia	Shangwan coal	#4	4.42	4.88	34.35	60.77	77.33	4.44	16.41	1.18	0.29
Inner Mongolia	Qihua coal	#5	4.11	12.51	31.74	55.74	77.82	4.29	17.28	1.18	0.45
Ningxia	Lingxin coal	#6	9.65	7.56	28.52	63.93	77.44	3.63	17.85	1.14	0.19
Ningxia	Yangchangwan coal	#7	8.36	10.53	28.18	61.29	76.00	3.60	20.32	1.02	0.40

reasonably predicted by this model. The model-predicted coal conversion profiles and temperature profiles during devolatilization in the pilot-scale plasma reactor are plotted in Figure 4. Figure 4 clearly shows that the fast release of volatiles is dominated by the rapid heating of the particle. Conversely, volatiles evolution would significantly influence the particle heating history. Therefore, the two-way coupling calculation is the premise and foundation for the accuracy of the predicted particle-scale devolatilization behaviors in a practical plasma reactor.

Effect of coal feed rate

The following discussion is based on the simulations that were carried out under the typical operating conditions (see Table 1, Coal #1) from the pilot-scale plasma reactor. For efficiency, life time, and stability reasons, the mass flow rate of hydrogen introduced into the plasma torch could not be changed arbitrarily (the optimal value is shown in Table 1). Therefore, only the coal feed rate varied from 400 to 1400 kg/h to clarify the effect of coal-hydrogen feed ratio in this work, with the basic assumption that coal particles were dispersed uniformly in the system. The variations of residence time, the average temperatures of gas and particles with coal feed rate are shown in Figure 5. The profiles of the average coal conversion, the mass flow rates of volatiles and char with coal feed rate are shown in Figure 6.

As shown in Figures 5 and 6, the coal feed rate has a significant impact on the final average gas temperature, particle temperature, coal conversion, and residence time. With the increase of the coal feed rate to this system, the total enthalpy/energy of the heating gas surrounding each particle would decrease as the total power input is constant. Therefore, a larger coal feed rate would lead to a lower final gas temperature and particle temperature, which causes the reasonable lower coal conversion and a longer time for completing devolatilization. The mass flow rate of total volatiles slightly increases with increasing coal feed rate, although the final coal conversion decreases remarkable. According to our previous work,[28] the optimal quench temperature was suggested to be in the range of 1700–1900 K. Thus, it can be concluded that the optimal mass flow rate of coal particles for this pilot-scale coal pyrolysis process is suggested to be 600–750 kg/h according to the simulation results shown in Figure 5. Under such optimized conditions, the final average particle temperature and final average coal conversion are in the range of 1550–1790 K and 43.5–45.8 wt %, respectively.

The variations of the maximum temperature difference and coal conversion difference inside particle as a function of residence time with different coal feed rates are plotted in Figure 7. The maximum coal conversion difference inside particle (i.e., ΔX), which represents the conversion gradient inside particle, is dominated by the temperature gradient inside particle. Both the peak values of the maximum temperature difference and coal conversion difference inside particle (which represents the temperature/conversion gradient inside particle) decrease but always exist with increasing coal feed rate. Correspondingly, the conversion gradient inside particle would disappear more slowly when the coal feed rate is larger. This is in conformity with the afore mentioned conclusion that the inherent resistances inside particle cannot be ignored. In case of 1400 kg/h coal feed rate, the average gas temperature would drop rapidly once it mixed with the coal stream. The driving force of heat transfer is also rapidly falling, leading to a relatively low temperature at the center of particle even in the outlet of reaction chamber (only reaches 1062 K). That is, the devolatilization is almost complete at the surface of particle (38 wt % daf) while inadequate at the center of particle (18.5 wt % daf). This is why there is a long tail in the ΔX vs. time curve for high coal feed flow rates. In case of 400 kg/h coal feed rate, the driving force of heat transfer is much larger so that the local temperatures at from the center to the surface of particle would reach the gas temperature before it reaches the outlet of the reaction chamber. Therefore, the devolatilization at any position of particle is complete. Therefore, the ΔX for the 400 kg/h case is large than that of the 1400 kg/h case in the first half of the chamber while the opposite phenomenon occurs in the second half of the chamber.

Effect of coal particle size

To reveal the influence of coal particle size, the coal diameter (Coal #1) varied from 10 to 200 μm while the other

Table 3. Chemical Structure Parameters of Coals for CPD Model

Coals			Chemical Structure Parameter					
Origin	Name	Number	p_0	c_0	$\sigma+1$	$M_{cluster}$	M_{del}	M_{sub}
Xinjiang	Heishan coal	#1	0.607	0.070	5.09	318.00	37.10	15.235
Xinjiang	Xinjiang coal	#2	0.601	0.066	5.11	320.96	37.55	14.951
Xinjiang	Miquan coal	#3	0.538	0.022	5.08	343.11	36.83	15.643
Inner Mongolia	Shangwan coal	#4	0.643	0.055	5.26	310.81	35.24	17.582
Inner Mongolia	Qihua coal	#5	0.669	0.067	5.28	298.23	34.00	16.408
Ningxia	Lingxin coal	#6	0.721	0.075	5.59	332.73	33.11	17.123
Ningxia	Yangchangwan coal	#7	0.742	0.109	5.61	335.46	34.17	14.836

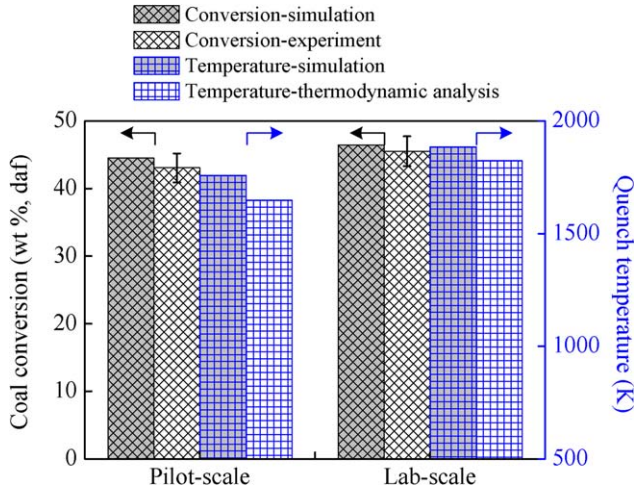

Figure 1. Comparisons of the model predictions with the corresponding experimental data and thermodynamic analysis results under the operating conditions from the 2000 kW pilot-scale and 10 kW lab-scale plasma reactors.

[Color figure can be viewed in the online issue, which is available at wileyonlinelibrary.com.]

operating conditions were assumed to be the same as those from the pilot-scale reactor shown in Table 1. Different particle sizes directly lead to different particle heating histories, and thereafter different coal devolatilization performances, and different final average temperatures of gas and particles as well, as shown in Figure 8.

With the increase of the coal particle diameter, the intensity of heat transfer between the heating gas and particles becomes weaker (the heat transfer quantity from gas to coal particles is 763 kW when the particle diameter is 40 μm while only 379 kW when the particle diameter is 140 μm) as the heat-transfer coefficient between the heating gas and particles decreases. Thus a larger coal particle would result in a lower final average coal conversion and a lower heat-transfer

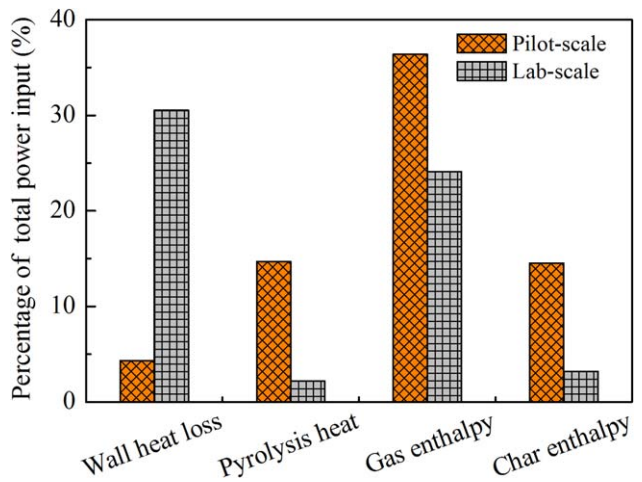

Figure 2. Energy balances around the reaction chamber of the pilot-scale and lab-scale plasma reactors.

[Color figure can be viewed in the online issue, which is available at wileyonlinelibrary.com.]

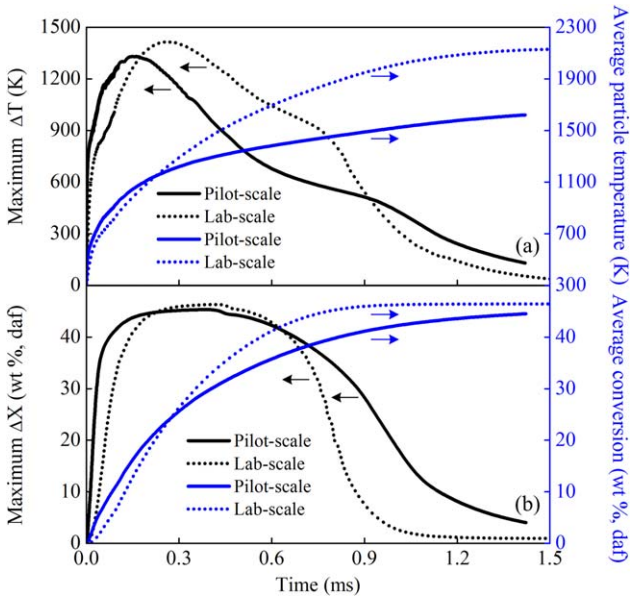

Figure 3. Variations of (a) maximum temperature difference inside particle and average particle temperature and (b) maximum coal conversion difference inside particle and average conversion with time under the typical operating conditions from the pilot-scale and lab-scale plasma reactors.

[Color figure can be viewed in the online issue, which is available at wileyonlinelibrary.com.]

quantity from gas to particles, leading to a higher final gas temperature but a lower particle temperature. The final average particle temperature would be even lower than 1000 K

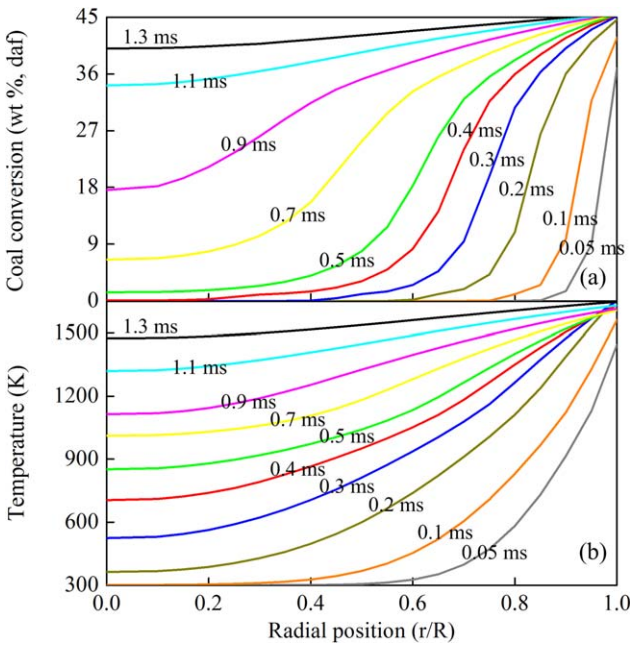

Figure 4. Predicted radial profiles of (a) coal conversion and (b) temperature at different time under the typical operating conditions from the pilot-scale plasma reactor.

[Color figure can be viewed in the online issue, which is available at wileyonlinelibrary.com.]

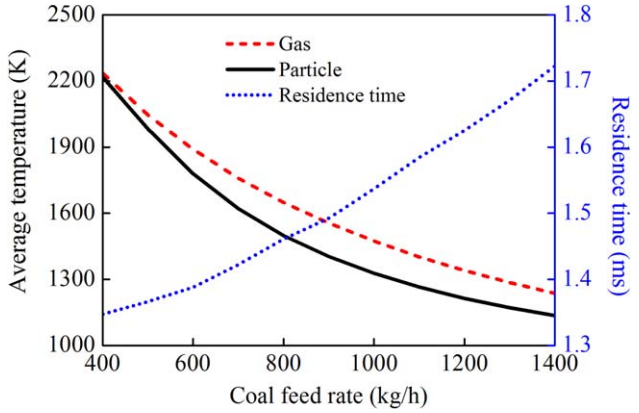

Figure 5. Effect of coal feed rate on residence time, the average temperatures of gas and particle under the typical operating conditions from the pilot-scale plasma reactor.

[Color figure can be viewed in the online issue, which is available at wileyonlinelibrary.com.]

and the corresponding average coal conversion is below 18 wt % when the particle diameter is larger than 140 μm. According to Figure 8, the optimal coal particle size for this process is suggested to be 40–50 μm. Under such optimized conditions, the average residence time is about 1.40 ms; the final average gas temperature and final average coal conversion are in the range of 1730–1760 K and 44.5–45.8 wt %, respectively.

Again, the variations of the maximum temperature difference and coal conversion difference inside particle as a function of residence time with different particle sizes are plotted in Figure 9. The disappearance of the temperature/conversion gradient inside particle (i.e., there is almost no temperature/conversion difference inside particle) means that the thermal equilibrium between the heating gas and particles is reached in the pilot-scale reactor. Thus it can be seen from Figure 9 that the energy/enthalpy contained in the heating gas would be comparatively well utilized when the particle diameter is smaller than 50 μm. There is a measurable reduction in the energy utilization efficiency when the particle diameter is

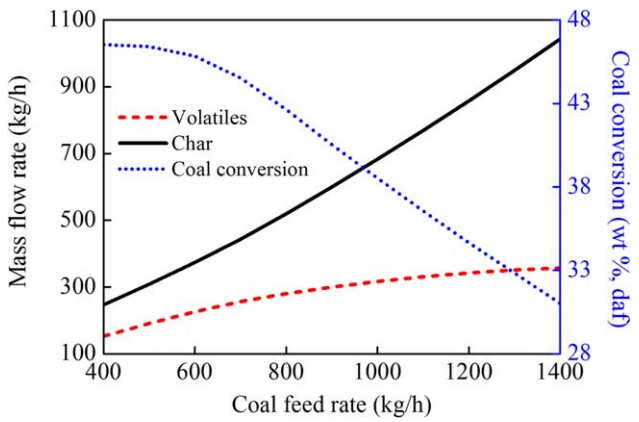

Figure 6. Effect of coal feed rate on coal conversion, the mass flow rates of volatiles and char under the typical operating conditions from the pilot-scale plasma reactor.

[Color figure can be viewed in the online issue, which is available at wileyonlinelibrary.com.]

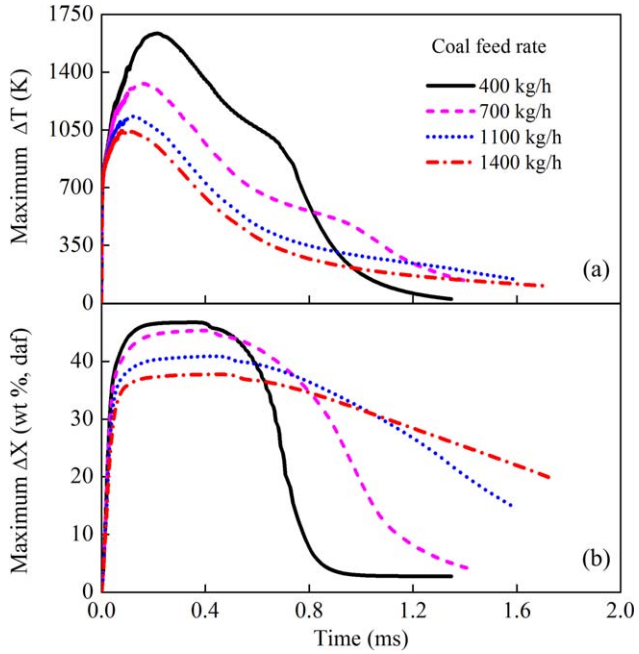

Figure 7. Variations of (a) maximum temperature difference and (b) maximum coal conversion difference inside particle with time at different coal feed rates under the typical operating conditions from the pilot-scale plasma reactor.

[Color figure can be viewed in the online issue, which is available at wileyonlinelibrary.com.]

larger. When the particle diameter is larger than 90 μm, heat could not be transferred efficiently into the center region of the coal particle due to the resistance of heat conduction. This results in the complete devolatilization in the surface shell but little reaction in the core of a particle, even at the outlet of the pilot-scale plasma reactor.

Selection of coal type

As is well known, the properties of coal feedstock are of great importance to the performance of the plasma reactor

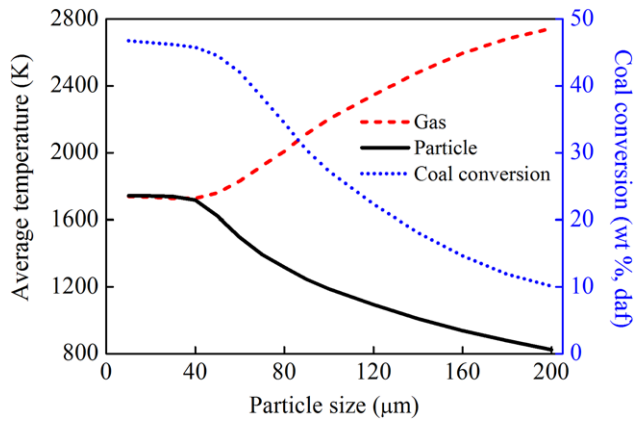

Figure 8. Effect of particle size on coal conversion, the average temperatures of gas and particle under the typical operating conditions from the pilot-scale plasma reactor.

[Color figure can be viewed in the online issue, which is available at wileyonlinelibrary.com.]

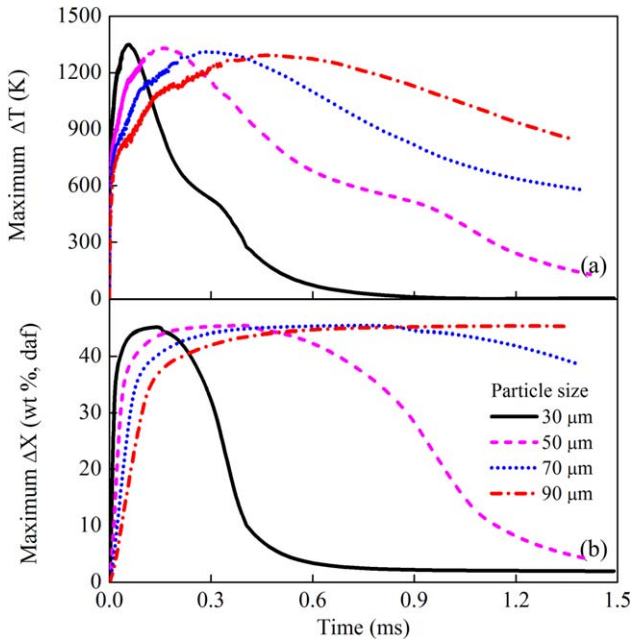

Figure 9. Variations of (a) maximum temperature difference and (b) maximum coal conversion difference inside particle with time at different particle sizes under the typical operating conditions from the pilot-scale plasma reactor.

[Color figure can be viewed in the online issue, which is available at wileyonlinelibrary.com.]

owing to the complex physical structure and chemical composition of coal. As this two-way coupling model has been proved to be capable of describing the pyrolysis behaviors in the practical plasma reactors of various coal types, the simulations can help to provide a simple, quick method of coal type selection for the industrial plasma technology, instead of testing the performance of all the coals in a complex plasma reactor under extreme conditions.

Therefore, a number of numerical experiments on the devolatilization behaviors of seven kinds of coals (including Coal #1) under the typical operating conditions from the pilot-scale plasma reactor were carried out. In these calculations, the coal feed rate (dried sample) and coal particle diameter were set to 700 kg/h and 50 μm, respectively. Tables 2 and 3 list the analytical data and the coal-dependent chemical structure parameters for the CPD model of the seven coal samples. The simulation results are shown in Table 4.

As shown in Table 4, the residence times of all coals are very close (in the range of 1.40–1.55 ms) while different coal properties directly result in different coal conversions and different mass flow rates of volatiles, leading to different final average temperatures of gas and particles. Generally speaking, the performance of the coal pyrolysis process is characterized by the mass flow rate of acetylene. The mass flow rate of acetylene could be estimated based on the final gas temperature, the mass flow rate, and the assumed composition of volatiles using thermodynamic approach. The conversions of H, O, N, and S elements in coal were reasonable estimated according to our previous work[19,28] for the seven coals. Then the conversion of C can be calculated according to the conversion of coal. Under above assumptions, the sequence in terms of reactor performance of the seven coals (Coal #3 > Coal #2 > Coal #1 > Coal #4 > Coal #5 > Coal #6 > Coal #7) was obtained based on the mass flow rate of acetylene.

It should be mentioned that although the CPD model has been successfully used to calculate the quantity of char, tar, and light gases products during pyrolysis, the composition of light gases evolved, however, have to be specified by the user. To accurately model the pyrolysis performance of those coals with very different chemical compositions requires the quantity and distribution of light gases (such as CH_4, CO_2, CO, H_2O, N_2, and other light gas species) during devolatilization. Therefore, a submodel used to estimate the composition of light gases during pyrolysis is expected to be developed and incorporated into the CPD model in the future work.

Conclusion

A generalized heat transfer and devolatilization model incorporating the mechanism of coal chemistry and particle-scale physics has been coupled with the thermal balance between the heating gas and coal particles to predict the coal pyrolysis behaviors in the practical plasma reactors where the temperature, components, and properties of the heating gas changes significantly during devolatilization.

This two-way coupling model was well validated with the experimental data from both the pilot-scale and the lab-scale plasma reactors, and proved to be capable of describing the complex coal pyrolysis behaviors in the practical plasma reactors. The overall energy balances of both reactors were analyzed. The results revealed that total heat content of products before quenching in the pilot-scale reactor was fairly high. Furthermore, the influences of coal feed rate and particle size on the reactor performance were carried out. The results showed that a larger coal feed rate or a larger particle size would weaken the intensity of heat transfer between the heating gas and particles, leading to a lower final particle temperature and thereafter a worse devolatilization

Table 4. Predicted Devolatilization Performances for Seven Coal Samples in the Pilot-Scale Plasma Reactor

Coals			Residence Time	Coal Conversion	Volatiles Mass Flow Rate	Yield of Acetylene	Gas Temperature	Particle Temperature
Origin	Name	Number	ms	wt %, daf	kg/h	wt %, daf	K	K
Xinjiang	Heishan coal	#1	1.42	44.5	256.3	17.5	1759	1621
Xinjiang	Xinjiang coal	#2	1.42	44.5	264.4	17.7	1759	1624
Xinjiang	Miquan coal	#3	1.40	47.4	291.4	22.8	1738	1572
Inner Mongolia	Shangwan coal	#4	1.47	37.6	250.3	12.5	1733	1615
Inner Mongolia	Qihua coal	#5	1.48	37.2	227.5	11.8	1769	1681
Ningxia	Lingxin coal	#6	1.54	29.9	193.7	5.0	1782	1728
Ningxia	Yangchangwan coal	#7	1.52	32.5	203.5	4.3	1784	1720

performance. The optimal values of coal feed rate and particle size were suggested to be 600–750 kg/h and 40–50 μm, respectively. Finally, the fresh numerical experiments on the devolatilization behaviors of several coals were performed together with the thermodynamic approach, providing a simple, quick method of coal type selection for industrial plasma technology.

All the simulations in this work are based on an important assumption that the particles are ideally mixed with the thermal plasma. However, ideal gas-particle mixing might fail in the commercial reactor so that the contact efficiency between the heating gas and coal particles is to be dominant. Therefore, it is anticipated that this model would be further integrated with the complex multiphase reacting flows for modeling coal pyrolysis in the practical plasma reactors.

Acknowledgments

Financial support from the National Basic Research Program of China (973 Program No. 2012CB720301), the National Natural Science Foundation of China (NSFC) under grant No. 20976091, the China Postdoctoral Science Foundation under grant No. 2014M550072, the National Institute of Clean-and-Low-Carbon Energy (NICE) and Xinjiang Tianye (Group) Co. Ltd. are acknowledged.

Literature Cited

1. Yan BH, Lu W, Cheng Y. China goes green: cleaner production of chemicals. *Green Process Synth.* 2012;1:33–48.
2. Yan BH, Cheng Y, Jin Y. Cross-scale modeling and simulation of coal pyrolysis to acetylene in hydrogen plasma reactors. *AIChE J.* 2013;59:2119–2133.
3. Bond RL, Ladner WR, Mcconnell GIT, Galbraith IF. Production of acetylene from coal, using a plasma jet. *Nature.* 1963;200:1313–1314.
4. Nicholson R, Littlewood K. Plasma pyrolysis of coal. *Nature.* 1972; 236:397–400.
5. Gannon RE, Krukonis VJ, Schoenbe. T. Conversion of coal to acetylene in arc-heated hydrogen. *Ind Eng Chem Process Des Dev.* 1970; 9:343–347.
6. Krukonis VJ, Gannon RE, Modell M. Deuterium and carbon-13 tagging studies of the plasma pyrolysis of coal. *Adv Chem Ser.* 1974; 131:29–41.
7. Chakravartty SC, Dutta D, Lahiri A. Reaction of coals under plasma conditions—direct production of acetylene from coal. *Fuel.* 1976;55: 43–46.
8. Bittner D, Baumann H, Klein J. Relation between coal properties and acetylene yield in plasma pyrolysis. *Fuel.* 1985;64:1370–1374.
9. Wang S, Chen HG, Xie KC. The effect of component of coal on the yield of acetylene in arc plasma pyrolysis. *Chem Ind Eng.* 2003;20: 195–199.
10. Cheng Y, Chen JQ, Ding YL, Xiong XY, Jin Y. Inlet effect on the coal pyrolysis to acetylene in a hydrogen plasma downer reactor. *Can J Chem Eng.* 2008;86:413–420.
11. Yan BH, Cheng Y, Xu PC, Cao CX, Cheng Y. Generalized model of heat transfer and volatiles evolution inside particles for coal devolatilization. *AIChE J.* 2014;60:2893–2906.
12. Grant DM, Pugmire RJ, Fletcher TH, Kerstein AR. Chemical-model of coal devolatilization using percolation lattice statistics. *Energy Fuel.* 1989;3:175–186.
13. Fletcher TH, Kerstein AR, Pugmire RJ, Grant DM. Chemical percolation model for devolatilization. 2. Temperature and heating rate effects on product yields. *Energy Fuel.* 1990;4:54–60.
14. Fletcher TH, Kerstein AR, Pugmire RJ, Solum MS, Grant DM. Chemical percolation model for devolatilization. 3. Direct use of C-13 NMR data to predict effects of coal type. *Energy Fuel.* 1992;6: 414–431.
15. Veras CAG, Carvalho JA, Ferreira MA. The chemical percolation devolatilization model applied to the devolatilization of coal in high intensity acoustic fields. *J Braz Chem Soc.* 2002;13:358–367.
16. Fletcher TH, Pond HR, Webster J, Wooters J, Baxter LL. Prediction of tar and light gas during pyrolysis of black liquor and biomass. *Energy Fuel.* 2012;26:3381–3387.
17. Patrick AJ Jr., Gannon RE. 1 MW prototype arc reactor for processing coal to chemicals. In: Cheremisinoff PN, Farah OG, Ouellette R, editor. Radio Frequency/Radiation and Plasma Processing. Lancaster, PA: Technomic Publishing, 1985:144–154.
18. Chen J, Cheng Y. Process development and reactor analysis of coal pyrolysis to acetylene in hydrogen plasma reactor. *J Chem Eng Jpn.* 2009;42:103–110.
19. Yan BH, Xu PC, Guo CY, Jin Y, Cheng Y. Experimental study on coal pyrolysis to acetylene in thermal plasma reactors. *Chem Eng J.* 2012;207–208:109–116.
20. Shurtz RC, Kolste KK, Fletcher TH. Coal swelling model for high heating rate pyrolysis applications. *Energy Fuel.* 2011;25:2163–2173.
21. Shuang Y, Wu CN, Yan BH, Cheng Y. Heat transfer inside particles and devolatilization for coal pyrolysis to acetylene at ultrahigh temperatures. *Energy Fuel.* 2010;24:2991–2998.
22. Spalding DB. Some Fundamentals of Combustion. London: Butterworths Scientific Publications, 1955.
23. Fogler HS. Elements of Chemical Reaction Engineering, 4th ed. New Jersey: Prentice Hall, 2006:473–478.
24. Badzioch S, Field MA, Gregory DR. Investigation of temperature variation of thermal conductivity + thermal diffusivity of coal. *Fuel.* 1964;43:267–280.
25. Merrick D. Mathematical models of the thermal decomposition of coal. 2. Specific heats and heats of reaction. *Fuel.* 1983;62:540–546.
26. Boulos MI, Fauchais P, Pfender E. Thermal Plasmas: Fundamentals and Applications, Vol. 1. New York: Plenum Press, 1994.
27. Kauzmann W. Kinetic Theory of Gases. New York: W.A. Benjamin, 1966.
28. Yan BH, Xu PC, Jin Y, Cheng Y. Understanding coal/hydrocarbons pyrolysis to acetylene in thermal plasma reactors by thermodynamic analysis. *Chem Eng Sci.* 2012;84:31–39.

Manuscript received June 24, 2014, and revision received Oct. 16, 2014.